Stage-dependency of apoptosis and the blood-testis barrier in the dogfish shark (*Squalus acanthias*): cadmium-induced changes as assessed by vital fluorescence techniques

Leon M. McClusky1

(1) Department of Physiology, Faculty of Health Sciences, University of Pretoria, P.O. Box 2034, Pretoria, South Africa

Abstract

Naturally occurring heavy metals and synthetic compounds are potentially harmful for testicular function but evidence linking heavy metal exposure to reduced semen parameters is inconclusive. Elucidation of the exact stage at which the toxicant interferes with spermatogenesis is difficult because the various germ cell stages may have different sensitivities to any given toxicant, germ cell development is influenced by supporting testicular somatic cells and the presence of inter-Sertoli cell tight junctions create a blood-testis barrier, sequestering meiotic and postmeiotic germ cells in a special microenvironment. Sharks such as *Squalus acanthias* provide a suitable model for studying aspects of vertebrate spermatogenosis because of their unique features: spermatogenesis takes place within spermatocysts and relies mainly on Sertoli cells for somatic cell support; spermatocysts are linearly arranged in a maturational order across the diameter of the elongated testis; spermatocysts containing germ cells at different stages of development are topographically separated, resulting in visible zonation in testicular cross sections. We have used the vital dye acridine orange and a novel fluorescence staining technique to study this model to determine (1) the efficacy of these methods in assays of apoptosis and blood-testis barrier function, (2) the sensitivity of the various spermatogonial generations in *Squalus* to cadmium (as an illustrative spermatotoxicant) and (3) the way that cadmium might affect more mature spermatogenic stages and other physiological processes in the testis. Our results show that cadmium targets early spermatogenic stages, where it specifically activates a cell death program in susceptible (mature) spermatogonial clones, and negatively affects blood-testis barrier function. Since other parameters are relatively unaffected by cadmium, the effects of this toxicant on apoptosis are presumably process-specific and not attributable to general toxicity.

Introduction

Although concerns continue to be expressed over the potential harmful effects of naturally occurring heavy metals and synthetic compounds on testicular function (Sundaram and Witorsch *1995*; Sever *1997*), evidence linking heavy metal exposure to reduced semen parameters is inconclusive (Hjollund et al. *1998*). However, the increased human use of the heavy metal cadmium, one of the most toxic testicular toxicants known, is of concern, because cadmium is known to alter the expression of a variety of proteins, from protooncogenes (Hechtenberg et al. *1996*) to testicular tight-junction-associated proteins (Chung and Cheng *2001*). Cadmium has long been known to have rapid degenerative (Chiqouine and Suntzeff *1965*; Xu et al. *1996*; Sinha Hikim et al. *1997*) and spermiation-failure effects (Hew et al. *1993a,b*) on the testis. The particular sensitivity of the testis to cadmium exposure may be related to the testis being a highly proliferative and acutely hormone-dependent organ. Recent evidence concerning the direct and indirect impairment, at low cadmium doses, of steroidogenic activities, with the subsequent induction of germ cell apoptosis (Ozawa et al. *2002*; Gupta et al. *2004*) are consistent with its endocrine disruptive actions in other tissues (Choe et al. *2003*; Vetillard and Bailhache *2005*).

Despite cadmium being significantly correlated with human semen volume and spermatozoa defects (Chia et al. *1992*) and accumulating in an age-dependent manner in the testes of men (Oldereid et al. *1993*), knowledge about its subtle effects on all testicular processes, from gonocytogenesis to spermiogenesis, is incomplete.

Whereas fertility and the number of sperm produced are, in the final analysis, the ultimate indicators of toxicant effects, elucidation of the exact stage at which the toxicant may interfere with spermatogenesis or any cell type may be difficult, because (1) the various germ cell stages and substages within any given germ cell stage may have different sensitivities to any given toxicant, (2) germ cell development occurs in the context of a complex three-dimensional intimate relationship with supporting testicular somatic cells, i.e. Sertoli, Leydig, and peritubular myoid cells (Jégou et al. *1992*; Grima et al. *1998*) and (3) the presence of inter-Sertoli cell tight junctions create an evolutionary conserved blood-testis barrier that sequestrates meiotic and postmeiotic germ cells into a special microenvironment (Dym and Fawcett *1970*; Bergmann et al. *1984*).

In accordance with recent trends, we have sought a model in which susceptible stage(s) and cell population(s) can be examined and assessed in their normal physiological context. Compared with other vertebrates, sharks such as *Squalus* and related species have a unique combination of features. First, they have a "cystic" mode of spermatogenesis, in which a single germinal clone and a second clonal population of stage-synchronized Sertoli cells form a follicle-like unit (spermatocyst). Second, since differentiated Leydig cells have not yet evolved at this phyletic level and are thus absent from the testis (Pudney and Callard *1984*), spermatogenesis relies exclusively, or mainly, on Sertoli cells for somatic cell support. Third, because spermatocysts are linearly arranged in a maturational order across the diameter of the elongated testis, spermatocysts containing germ cells at different stages of development are topographically separated, resulting in a readily visible zonation in testicular cross sections. Several zones of maturation are easily distinguishable on the basis of their transillumination characteristics, colour and position relative to the germinal zone (GZ, the folliculogenic cyst-producing germinal ridge running the length of the testis) and the epigonal organ (a lymphomyeloid tissue mass encapsulating the mature pole of the testis). Testicular activity follows a protracted seasonal cycle that includes a winter period of spermatogenic arrest, such that upon resumption of spermatogenic activities in the spring, the previous season's mature spermatogonial spermatocysts are condemned to apoptotic death, resulting in a zone of degeneration (ZD) at the spermatogonia/spermatocyte transition in spermatogenically active *Squalus* (McClusky *2005*).

These anatomical features in *Squalus* have been used to show that proliferative activity, as measured by [^{3}H]thymidine incorporation (DuBois and Callard *1991*, *1993*) and proliferating cell nuclear antigen (PCNA) immunoexpression (McClusky *2005*), and DNA fragmentation, as measured by the DNA ladder assay (Callard et al. *1995*) and in situ end-labelling detection of DNA fragments (McClusky *2005*), are limited to the premeiotic (PrM, spermatogonia, preleptotene spermatocytes) region of the shark testis. A well-known mammalian spermatoxicant, cadmium (Cd^{2+}), has also been shown to preferentially accumulate in the PrM region of the shark testis within 3 days of a single cadmium injection (Betka and Callard *1999*).

As a first step in developing an in vivo test system for toxicological studies, we have therefore sought to develop valid techniques for assessing stage-specific functions in living testicular tissue by using this model. The use of vital staining techniques to assess these processes obviates the need for fixation and tissue-processing. One such technique involves the use of the vital dye acridine orange (AO), which specifically labels free and phagocytosed apoptotic corpses and metabolically competent cells exhibiting pyknosis or containing condensed chromatin, whereas necrotic cells are unlabelled (Abrams et al. *1993*; Broaddus et al. *1996*). In a comparison of several techniques (DNA laddering, annexin V staining, mitochondrial potential changes, caspase activity, flow cytometry, vital staining with the fluorescent dyes Hoechst 33342 and AO) to detect apoptosis in cultured cells, AO has been found to detect

apoptosis the earliest, even before caspase activation (Durrieu et al. *1998*). We also report a novel fluorescence staining technique to assay for a functional blood-testis barrier, during which intact inter-Sertoli cell tight junctions exclude the 10,000 MW rhodamine-labelled dextran molecule. The aims of the present study have therefore been to determine (1) the efficacy of these fluorescent stains to assay rapidly for at least two major processes during spermatogenesis in *Squalus*, i.e. apoptosis and blood-testis barrier function, (2) the utility of these techniques and this model to assess the sensitivity of the various spermatogonial generations in *Squalus* to cadmium (as an illustrative spermatotoxicant) and (3) the way that cadmium might affect more mature spermatogenic stages and other physiological processes in the testis.

Materials and methods

Animals and reagents

Twenty-five mature male spiny dogfish, *Squalus acanthias* (1.06–2.18 kg; 36–49 cm snout-vent length), were captured by a fishing boat of the Mount Desert Island Biological Laboratory at Salsbury Cove (Maine, USA) in the Gulf of Maine (USA) during the period of spermatogenic activity (June - August). Routine procedures at the Mount Desert Island Biological Laboratory included transferrance of the animals to husbandry facilities consisting of large natural seawater tanks, after which the animals were allowed to acclimatize for at least 2 days before experimentation. Animals (n=3–4/treatment group) were injected via the caudal vein either with elasmobranch dissecting medium (EDM: 280 mM NaCl, 10 mM HEPES, 5.5 mM d-glucose, 5.3 mM KCl, 0.44 mM KH_2PO_4, 0.18 mM $NaHCO_3$, 0.33 mM $Na_2HPO_4 \cdot 7H_2O$, 350 mM urea, pH 7.2) or with $CdCl_2$ (5 mg/0.2 ml EDM per kg body weight). This treatment elevates intratesticular cadmium levels by more than 150-fold and induces a more than 1.5-fold increase in metallothionein-like testicular cadmium-binding protein (Betka and Callard *1999*). Following injection, animals were maintained in running seawater tanks for 1 day (Exp. 1) or 3 days (Exp. 2) post-injection and then killed by double-pithing via the olfactory canal. Cadmium-treated and vehicle-treated animals were housed in separate tanks. In both experiments, which were conducted 1 week apart in July, controls were animals taken from the same collection cohort.

EDM and all other media and reagents were prepared with chemicals purchased from Sigma (St. Louis, Mo.), unless stated otherwise. Elasmobranch culture medium (ECM, pH 7.2) was phenol-red-free serum-free Leibowitz medium (GIBCO, Grand Island, N.Y.), adjusted for NaCl (280 mM) and urea (350 mM), HEPES (20 mM), penicillin (100 units/ml), streptomycin (100 μg/ml) and amphotericin B (250 μg/ml). AO was prepared just before use (500 μg/ml sterile water). Propidium iodide (PI) was prepared as a 100× stock solution (800 μg/ml sterile water), which was stored in aliquots at −20°C and thawed as needed. Dextran-rhodamine (D-R; 10,000 MW) was purchased from Molecular Probes/Invitrogen (Eugene, OR) and a l00× stock (25 mg/ml sterile water) was stored in aliquots at −20°C and thawed as needed. [³H]Thymidine (specific activity, 85 Ci/mmol) was purchased from New England Nuclear (Boston, Mass.). Optifluor scintillation cocktail was from Packard (Meriden, Conn.). All other chemicals were reagent grade.

Dissected cross sections and isolation of staged spermatocysts

At dissection, the testes were placed into iced sterile culture dishes and kept at 4°C during processing. As previously described (McClusky *2005*), cross sections (3–5 mm thick) were cut from the central third of each testis; two sections were fixed in 10% neutral buffered formalin (formaldehyde diluted 1:10 in EDM) at 4°C for 24 h, another section was placed in EDM for visualizing fluorescence characteristics of spermatocysts in situ and the remaining sections were used to isolate staged spermatocysts. Procedures for spermatocyst dispersal and culture have been previously described and validated (DuBois and Callard *1991*). In brief, dissected cross sections were separated into three major zones comprising

spermatocysts in premeiotic (PrM: spermatogonia and preleptotene spermatocytes), meiotic (M: primary and secondary spermatocytes, early round spermatids) and postmeiotic (PoM: elongating and mature spermatids) stages. Tissues from like stages were pooled, razor-minced and repeatedly washed in EDM with heparin (0.2 units/ml) and DNAase (15 Kunitz units/ml) to reduce reaggregation of released spermatocysts. This was followed by three washes in EDM containing bovine serum albumin (2.5 mg/ml) alternated with sedimentation at unit gravity. Cysts were finally resuspended in ECM (1:15; 1 ml packed cysts to 14 ml ECM), seeded in 350:l aliquots in Falcon 24-well plates (Becton Dickenson, Lincoln Park, N.J.) and cultured for the time specified.

Fluorescence microscopy

AO and PI staining   Freshly cut cross sections were floated on two layers of cheese cloth in ECM containing AO (5 μg/ml) in Falcon 12-well tissue culture plates at room temperature (RT) for 15–20 min. When used as a vital stain, AO labels metabolically competent apoptotic cells as bright green punctate fluorescence spots, whereas dead or necrotic cells stain unremarkably and weakly diffuse green (Abrams et al. *1993*; Broaddus et al. *1996*). By contrast, PI is excluded from living cells but readily enters the nucleus of dead cells or those in the final stages of apoptosis. Dispersed cysts were stained either with AO (0.1 μg/ml; 15 min) or PI (8 μg/ml; 30 min) at RT. For double-staining, cysts were first stained with PI for 30 min and then with AO for a further 15 min. After two washes, the sections or cysts were placed in fresh ECM and viewed under an Olympus IMT-2 inverted microscope fitted with epifluorescence (IMT2 DMB dichroic mirror at 490-nm excitation and 515-nm emission maxima for AO; and IMT2 DMG dichroic mirror at 545-nm excitation and 590-nm emission maxima for PI). A Hamamatsu charge-coupled device camera (model C2400; Hamamatsu Photonics Systems, Bridgewater, N.J.) relayed fluorescence microscopic images to a SONY monochrome video monitor (SONY Electronics, San Jose, Calif.) linked to a Power Macintosh computer equipped with an AG-5 frame grabber card (Scion, Frederick, Md.) and NIH Image (version 1.60) software. By using a 10x objective, live images of 7–8 fields of view of the complete spermatogenic sequence from immature to mature regions of AO-stained cross sections and of 6–10 fields of view of each replicate AO-stained or PI-stained well of dispersed spermatocysts (~50 cysts per field of view) were captured and stored for later analysis. Double-stained cysts were viewed by using filters for AO fluorescence and photographed by using Fujichrome 100 Provia Professional color reversal film.

D-R staining   To assess blood-testis barrier function by exclusion of 10,000 MW rhodamine-labelled dextran (D-R), seeded spermatocysts were incubated in duplicate wells for 1 h at RT in ECM containing 250 μg/ml D-R, washed with EDM (4×), placed in fresh ECM and viewed under the fluorescence microscope (IMT2 DMG dichroic mirror; 545-nm excitation and 590-nm emission maxima). Viability of cysts was measured simultaneously by incubating a set of duplicate wells of the same preparations with PI as described above. Images of five fields of view (6.3× objective; 35 cysts/field) of each well were captured and stored on computer.

Tissue preparation for immunohistochemistry

Procedures were as previously described (McClusky *2005*). Briefly, formalin-fixed tissues were washed twice in EDM (1 h each), stored in cold 70% ethanol for no longer than 3–5 weeks and embedded in Paraplast X-TRA (Oxford Labware, St. Louis, Mo.). Two consecutive 6–μm-thick sections were collected on slides pre-coated with poly-L-lysine (1 mg/ml, MW 335,000; Sigma) and allowed to air-dry. Sections were then deparaffinized and rehydrated stepwise through an ethanol series.

PCNA immunohistochemistry

PCNA immunostaining procedures were as previously described (McClusky *2005*) and were carried out with the Unitect Avidin-Biotin-Peroxidase immunohistochemistry Detection System Kit (Oncogene Science, Cambridge, Mass.) containing the recombinant PCNA mouse monoclonal PC10 antibody shown to interact with fish PCNA antigen (Ortego et al. *1994*). In brief, endogenous peroxidase was quenched by treating sections in darkness for 10 min with 3% hydrogen peroxide. Following a rinse in distilled water, the sections were subjected to an antigen retrieval procedure (Ortego et al. *1994*) that involved heating the sections in a microwave oven (450 W) in 1% anhydrous zinc sulphate for 3 min, resting for 1 min, and heating for a further 3 min. After being cooled for 15 min, sections were rinsed in distilled water and placed in 0.5% Tween 20 in phosphate-buffered saline (PBS-A: 137 mM NaCl, 29 mM $NaH_2PO_4 \cdot H_2O$, 9 mM Na_2HPO_4, pH 7.4) for 5 min. Sections were then incubated with 3.6% normal horse serum for 30 min at RT to reduce non-specific binding and then overnight at 4°C with PCNA antibody diluted 1:200 (final concentration 1 μg/ml) in Tween 20/PBS-A. After three washes in PBS-A, sections were incubated with biotinylated horse secondary antibody for 30 min at RT, washed in PBS-A and then incubated with the avidin-biotin-complex (ABC) for a further 30 min at RT. Following a 30-s rinse in 1% Triton X-100/PBS-A to reduce background staining, the antigen was finally detected by treating the sections for 3 min with 3,3′-diaminobenzidine (DAB; Vector, Burlingame, Calif.; positive cells were stained brown). Sections were counterstained with 0.5% methyl green in 100 mM sodium acetate (pH 4), dehydrated in 100% butanol, cleared in toluene and mounted with Permount (Fisher, Fair Lawn, N.J.). Negative controls were generated by substituting the primary antibody with the kit-supplied trp E antibody (0.5 μg/ml) and by serial dilution of the primary antibody. Each cyst was scored separately for PCNA-labelled germ cells or Sertoli cells; if at least 50% of nuclei of a given cell type in a cyst was PCNA-immunoreactive, the cyst was considered PCNA-positive (not all cells in a clone were precisely synchronized).

TUNEL immunohistochemistry

TUNEL staining procedures were as previously described (McClusky *2005*) and were carried out by using the ApopTag-Peroxidase Kit (Chemicon, Temecula, Calif.). Briefly, deparaffinized rehydrated sections were treated with 0.1% Triton X-100 in 0.1% sodium citrate for 3.5 min at RT and washed twice with PBS-B (50 mM sodium phosphate pH 7.4, 200 mM NaCl). Endogenous peroxidase was quenched by treating sections in darkness with 3% hydrogen peroxide for 10 min, followed by two washes in PBS-B. Subsequent steps were according to the supplier's instructions, except that the terminal transferase enzyme (TdT) was diluted 1:16 with sterile water. Following incubation of the sections with the TUNEL reaction mixture in a humidified chamber at 37°C for 1 h, sections were treated with the antidigoxigenin-peroxidase complex for 30 min at RT, followed by DAB, and then counterstained and mounted as described for PCNA. To generate negative controls, TdT was replaced with sterile water, whereas for positive controls, sections were pretreated with DNAse I (Sigma; 10 μg/ml in distilled water) to generate DNA fragments. For TUNEL scoring, spermatocysts that contained three or more TUNEL-positive cells were considered to be apoptotic, a standard previously used (McClusky *2005*).

DNA synthesis

[^{3}H]Thymidine (5 μCi/ml final concentration) was added at seeding to PrM cysts (cell-cycle activity is limited to PrM stages; McClusky *2005*). After 24 h, cysts were washed twice with EDM containing radio-inert thymidine (5 μg/ml) and the incorporation of [^{3}H]thymidine into acid-insoluble macromolecules was measured after trichloroacetic acid precipitation (DuBois and Callard *1991*, *1993*). Results were normalized for cyst protein (Lowry et al. *1951*).

Microscopy and data analysis

For analysis of apoptosis in PrM and ZD cysts (M and PoM stages were not apoptotic; McClusky *2005*), the diameters of all cysts in a field of view were measured, each cyst was scored as either AO-positive or AO-negative and the number of AO-positive spots per cyst was recorded. A cyst was designated AO-positive if it contained three or more bright green punctate fluorescent spots, a standard previously used (McClusky *2005*). Since the male *Squalus* population is not exactly synchronized in terms of spermatogenic activities, the ZD may be present at different stages of its formation among males. Large spherical ZD cysts (turgid condemned cysts) were scored but atrophied or flattened ZD cysts (terminal stages of condemned cysts) were excluded from analysis. The number of AO-positive spots in ZD cysts was arbitrarily designated as more than 100, because it was impossible accurately to count the large number of spots present in these cysts or to distinguish individual nuclei within multinucleate giant cells. Based on the measured diameters of cysts in fresh-cut cross sections and on comparison with criteria established for cysts in fixed and stained sections in an earlier report (McClusky *2005*), those cysts containing spermatogonia were divided into five substages: GZ stage, containing primary spermatogonia (<50 μm) and early stage PrM I (50-100 μm); early-stage PrM II (100–150 μm); mid-stage PrM I (150–200 μm); and mid-stage PrM II (200–250 μm), all with secondary spermatogonia. Data are presented as the mean percentage (±SEM) of AO-positive cysts or the mean number (±SEM) of AO-positive spots in each cyst-size class per treatment group. The mean percentage of PI-positive cysts (cysts with three or more bright red fluorescent spots) was determined as for AO. D-R exclusion was reported as the mean percentage cysts (±SEM) in each size or stage category.

Cyst counts for the quantification of PCNA and TUNEL immunostaining were performed as previously described (McClusky *2005*). Briefly, all cysts along three lines radiating from the germinal ridge to the proximal border of the mature testicular pole were counted, classified by stage and scored for PCNA or TUNEL immunoreactivity (total per animal=240–300 cysts). Since the developmental progression is accompanied by changes in cyst diameter, cyst counts were adjusted for the width of a testicular cross section at the midpoint of the segment occupied by each stage as follows:

$$N_{cyst}, xa = tw/d_{cyst} * l_{count},$$

where, N_{cyst}, xa is the number of cysts /cross-sectional area per stage, tw is the testis width at the midpoint of each cyst stage (in μm), d_{cyst} is the mean diameter of each cyst stage (in μm) and l_{count} is the mean number of cysts counted on three radiating lines at each stage.

Electron microscopy

To validate the use of AO vital staining for the detection of apoptosis, individual AO-positive PrM and ZD spermatocysts were collected with a micropipette and processed for electron microscopy. After fixation in glutaraldehyde and postfixation in osmium tetroxide, the cysts were dehydrated and embedded in an Epon/Araldite mixture. Thin sections were cut on a Porter-Blum Mark 2 ultramicrotome, stained sequentially in a saturated aqueous solution of uranyl acetate and 0.2% lead citrate and examined in a Jeol 100S electron microscope.

Statistics

Data are expressed as the mean percentage of AO-positive cysts, PI-positive cysts, D-R excluding cysts, cysts with PCNA-labelled germ cells, PCNA-labelled Sertoli cells, and TUNEL-labelled germ cells at each cyst substage. All raw percentage data have been arcsine-square-root transformed prior to analysis by one-way and two-way analysis of variance (ANOVA) by using SigmaStat, Version 2.0 (Jandel Scientific, San Rafael, Calif.). The Student-Newman-Keuls multiple comparisons test was used to determine which values differed significantly ($P<0.05$).

Results

Identification of apoptotic germ cells in living spermatocysts

AO vital staining of living testicular cross sections facilitated visualization of the maturational order of spermatocysts comprising the spermatogenic sequence in *Squalus*, from the stroma-rich GZ containing the most immature cysts to the mature pole containing the PoM cysts (Fig. 1). Most striking of all was the band of intensely yellow-green fluorescent cysts, comprising the ZD interposed between the PrM region and the AO-negative M stage region in spermatogenically active *Squalus*. When the ZD was visible as a wide band of highly fluorescent cysts, the ZD cysts were spherical and stained bright yellow-green (Fig. 1).
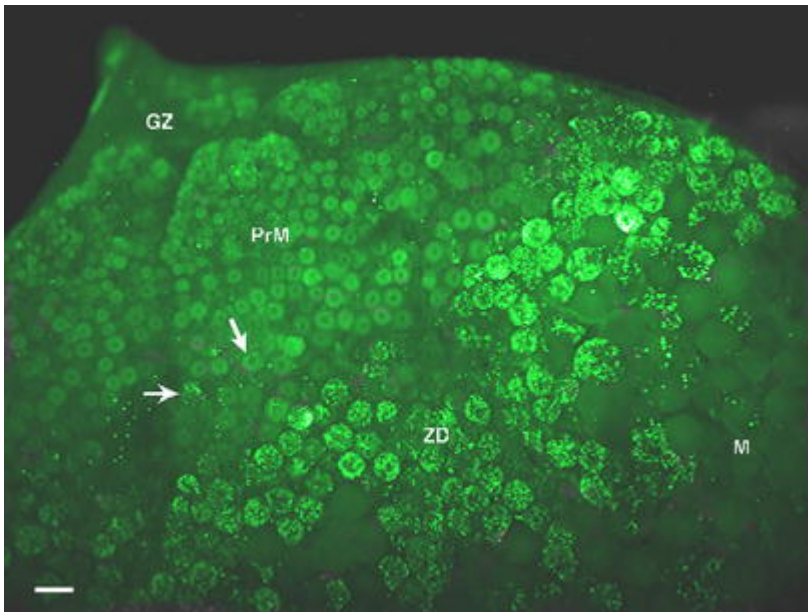
Fig. 1 Fluorescence-microscopic image of living spermatocysts in a freshly cut testicular cross section after acridine orange (AO) staining. AO, a vital nucleophilic dye, reveals chromatin condensation of apoptotic cells as punctate bright green fluorescence. The original microscopic image has been converted from grey-scale to colour by using Adobe Photoshop Version 4. GZ cysts are uniformly AO-negative. Whereas the majority of PrM cysts are unlabelled, increased incidence of specific AO-labelling are found in larger PrM cysts (*arrows*) adjacent to the heavily AO-labelled ZD cysts. At this time of year (early June), the thick layered ZD represents the previous season's mid-stage PrM cysts that have aborted their development. M stage cysts are uniformly AO-negative. *Bar* 400 μm

Conversely, the ZD was narrow in some animals, in which case the ZD cysts were oval or flattened and stained bright orange. Whereas all cysts in the GZ and meiotic regions were AO-negative and stained diffuse green, many PrM cysts found nearer to the ZD contained clusters of punctate bright green fluorescent spots (Fig. 1). Specific AO-labelling of such PrM cysts revealed an increasing gradient of AO-positive cysts in the PrM region (immature<mature). Mature PoM cysts also fluoresced intense bright green, with this AO-labelling being specifically associated with the spermatid heads (see Fig. 2).
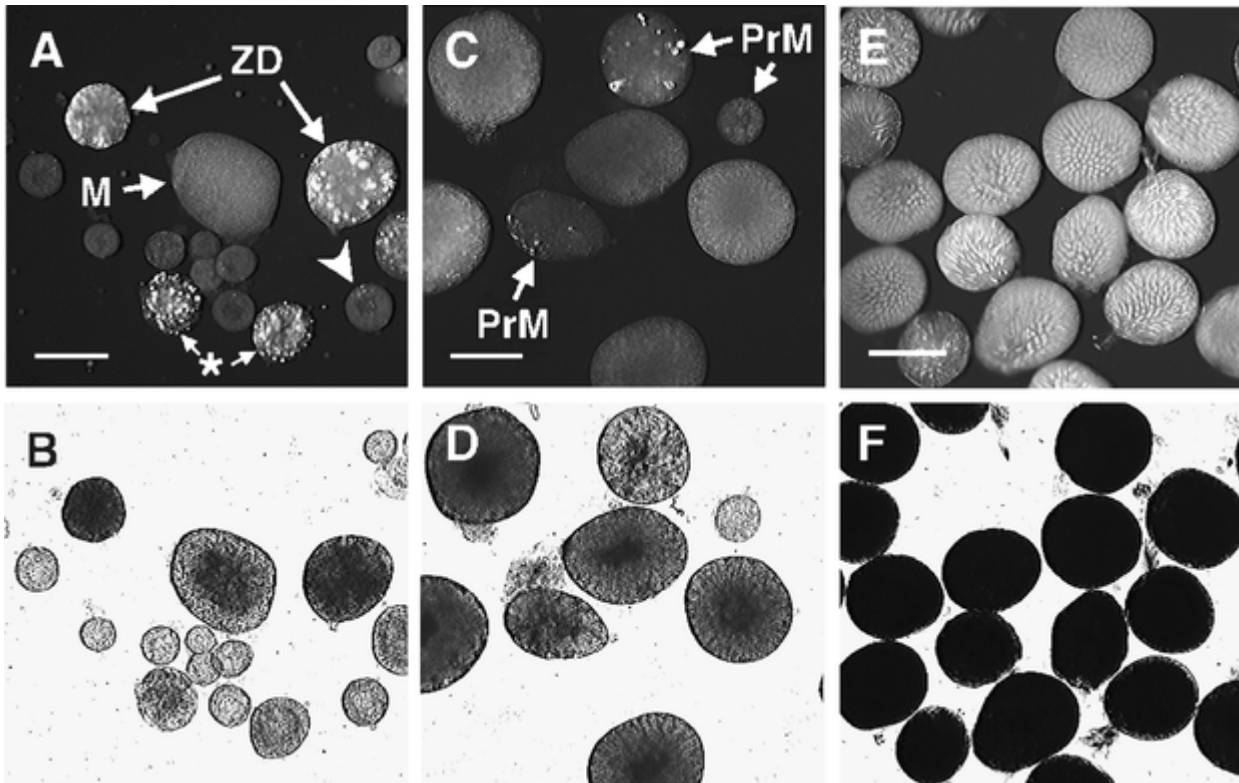
Fig. 2 Fluorescence-microscopic (**a**, **c**, **e**) and corresponding phase-contrast (**b**, **d**, **f**) images of AO-stained dispersed spermatocysts showing the cyst-size heterogeneity and AO-fluorescence staining characteristics of all stages. Dispersed cysts prepared from macroscopically staged PrM (**a**, **b**), M (**c**, **d**) and PoM (**e**, **f**) regions of the testis are shown. Small early-stage PrM cysts (**a**, **c**) are unlabelled, but larger mid-stage PrM cysts are heavily AO-labelled (*asterisk*) or have a few AO spots (*arrowhead*). ZD cysts (**a**) are intensely labelled with punctate AO spots, but M-stage (**c**) and PoM (**e**) cysts have no such spots. In contrast to the translucent phase-contrast appearance of small PrM cysts (**b**), corresponding phase-contrast images of heavily AO-labelled PrM (**a**), ZD (**a**) and PoM (**e**) cysts show a mottled (**b**, PrM) to a phase-dark appearance (**a**, ZD; **f**, PoM) indicating the presence of condensed chromatin. *Bar* 250 μm

Upon dispersal of cysts, the translucent phase-contrast appearance of small PrM cysts correlated with diffuse green AO fluorescence (Fig. 2a). By contrast, AO-staining of some larger PrM cysts revealed punctate bright green fluorescent spots, which correlated with a mottled phase-contrast appearance (Fig. 2a–d). AO-stained ZD cysts, which were filled with punctate bright yellow/orange fluorescent spots, had a phase-dark appearance (Fig. 2a,b). AO-staining of M-stage cysts resembled the diffuse green staining of small-sized PrM cysts, but their phase-contrast appearance was characterized by a central phase-dark area surrounded by a translucent peripheral area (Fig. 2a,b). M-stage cysts lacked punctate AO-labelling and fluoresced diffuse green (Fig. 2a,c), Since cysts grouped as M-stage cysts included those that contained spermatocytes and round spermatids, the transillumination patterns of M-stage cysts were variable with the central phase-dark area being larger in some M-stage cysts than in others (Fig. 2b,d). AO-staining of mature PoM cysts revealed the bright green fluorescing bundles of spermatid heads, which correlated with a total phase-dark appearance (Fig. 2e,f). These results indicated that intense bright green AO fluorescence was correlated with a phase-dark transillumination pattern and clearly suggested the chromatin in spermatids was condensed. Since condensed chromatin is not a feature of normal scheduled premeiotic activities, we concluded that specific AO-labelling in PrM and ZD cysts indicated chromatin condensation associated with apoptosis.

Electron microscopy of AO-positive cysts

To confirm the specificity of AO-labelling of apoptotic germ cells, PrM and ZD cysts containing punctate bright green/yellow AO fluorescent spots were individually selected and processed for electron microscopy. In PrM cysts, healthy spermatogonia were arranged in characteristic chains (Fig. 3a). Scattered among these chains of spermatogonia were single isolated, pyknotic and shrunken spermatogonia. ZD cysts lacked normal cellular organization, were filled with vacuolated spaces and contained many shrunken nuclei and germ cell corpses (Fig. 3b). These ultrastructural observations verified the specific AO-labelling of apoptotic spermatocysts and confirmed AO vital staining as a valid apoptosis assay in this system.
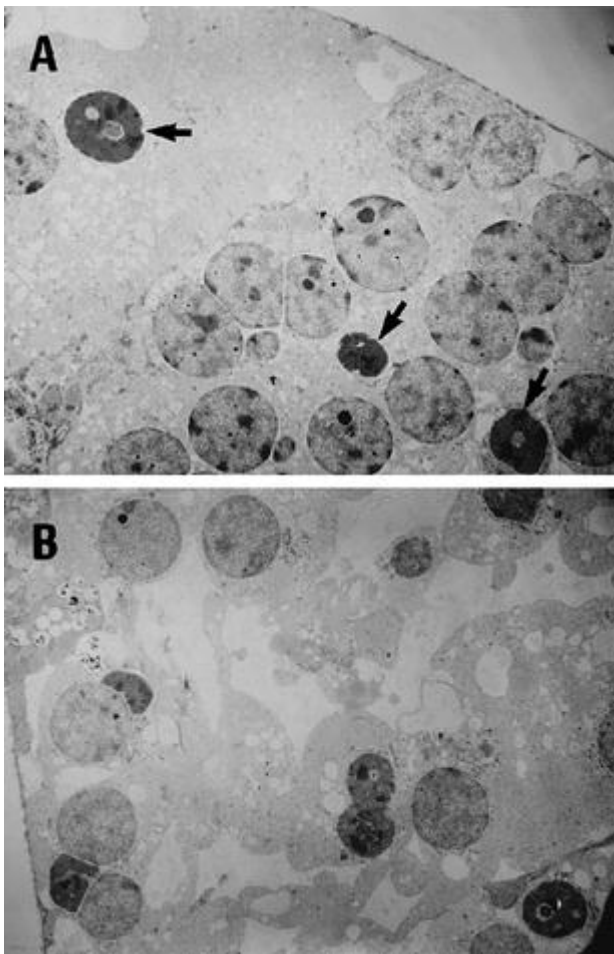
Fig. 3 Electron micrographs of an AO-positive PrM (**a**) and ZD cyst (**b**). **a** Nuclei (*arrows*) with electron-dense chromatin, typical of apoptotic nuclei. Note the chain-like arrangement of normal spermatogonia. **b** ZD cyst characterized by the lack of cellular organization and vacuolated spaces surrounding germ cell corpses. ×1,580

## AO and PI double-stained PrM cysts

Upon double-staining of PrM and ZD cysts with AO and PI, healthy PrM (Fig. 4a), partially AO-labelled PrM (Fig. 4b) and heavily AO-labelled ZD cysts (Fig. 4c) all excluded PI. Occasionally, some PrM cysts contained both AO-positive and PI-positive cells (Fig. 4d). These results demonstrated the utility of AO and PI in the detection of the various phases of the apoptotic death process.
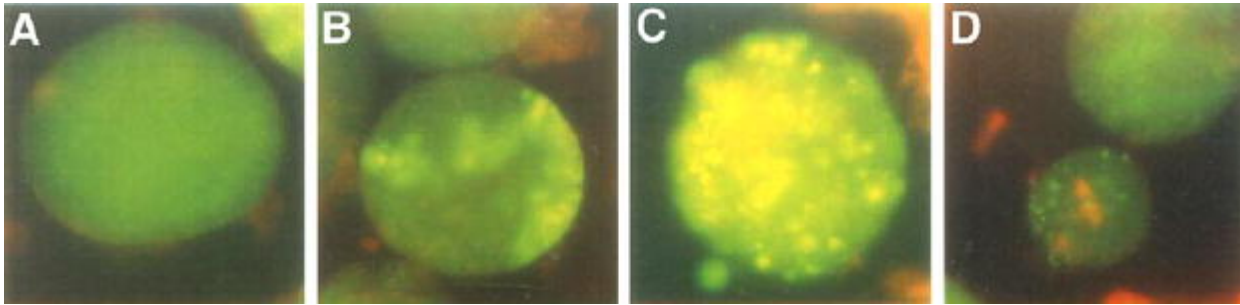
Fig. 4 Photomicrographs of PrM (**a**, **b**, **d**) and ZD (**c**) cysts double-stained with AO and PI, which label distinctly different stages of the degeneration process. Whereas healthy germ cells in a PrM cyst (**a**) stain collectively diffuse *green*, apoptotic cells are visible as punctate bright *green* fluorescent AO spots (**b–d**). In **c**, Sertoli cell phagocytosis of apoptotic corpses in a ZD cyst still precludes labelling of the corpses with PI, whereas dead germ cells prior to their phagocytosis are visible as bright *red* fluorescent spots (**d**). ×74

Stage-dependency of blood-testis barrier function

In order to assess whether the blood-testis barrier was functional, dispersed PrM, M and PoM cysts were incubated for 1 h in 10,000 MW D-R and their ability to exclude D-R was determined by fluorescence microscopy. Whereas D-R readily infiltrated all PrM cysts (Fig. 5b) and, to a lesser extent, M-stage cysts (Fig. 5c), total D-R exclusion was frequently and only observed in PoM cysts (Fig. 5a). Since the cysts comprising the PoM region included cysts at various stages of spermiogenesis, the extent of D-R exclusion was obviously dependent on the stage of spermiogenesis. Thus, some PoM cysts exhibited distinctly focal rhodamine fluorescence along the basement membranes of the cysts, such that these cysts appeared to be D-R permeant (Fig. 5a). However, at a different plane of focus on the surface of these cysts, accumulated D-R at the bases of the Sertoli cells defined the outlines of the large cell bodies of the Sertoli cells and thus created the peripheral focal areas of rhodamine fluorescence (Fig. 5a).
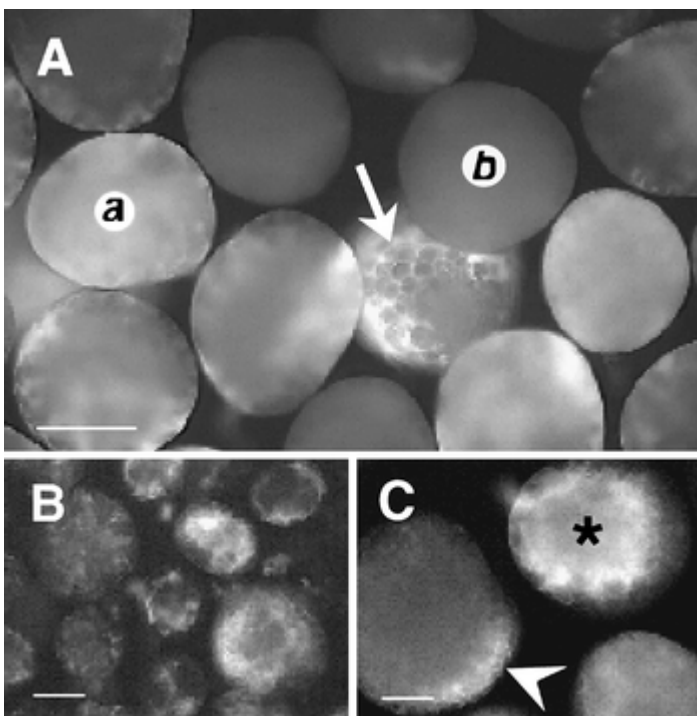

Fig. 5 Fluorescent-microscopic images of living cysts showing dextran-rhodamine (D-R) exclusion as a measure of blood-testis barrier function. Cysts harvested from the PoM region include D-R permeant (**a**) and D-R impermeant (**b**) cysts. At a different plane of focus on the surface of one impermeant cyst (*arrow*), D-R accumulates at the bases of Sertoli cells and outline the cell bodies of the Sertoli cells, all of which indicates the presence of inter-Sertoli tight junctions. All PrM cysts are readily permeant to D-R (**b**). Cysts harvested from the M region (**c**) include permeant (*asterisk*) and some partially permeant (*arrowhead*) cysts. Bars 150 μm (**a**), 100 μm (**b**, **c**)

Effects of cadmium on premeiotic events

To assess the regulation of spermatogonial cell kinetics through experimental manipulation, animals were injected with a single dose of cadmium (5 mg/kg) and killed after 1 or 3 days. In untreated animals, the percentage of AO-positive cysts in the PrM region varied significantly according to cyst size (size class in μm: [200–250]=[150–200]>[50–100]=[<50], $P<0.05$). At 1 day post-treatment, significant differences in the percentage of AO-positive cysts among the three treatment groups ($P<0.001$) and among the different cyst-size classes ($P<0.0001$) were noted (Exp. 1; Fig. 6). Although the overall interaction between treatment and cyst-size class was not significant ($P<0.2$), a 1-day cadmium treatment significantly increased the percentage of AO-positive cysts in the 150–200 μm size class by more than two-fold compared with vehicle-treated animals ($P<0.05$), with no changes in the percentage of PI-positive cysts or mean number of AO spots (Exp. 1, Fig. 6).

At 3 days post-treatment, differences in the percentage of AO-positive cysts, both among the three treatment groups and among the different cyst-size classes were significant ($P<0.0001$, Exp. 2, Fig. 6). The interaction between treatment and cyst-size class was significant ($P<0.004$). A 3-day cadmium treatment significantly ($P<0.05$) increased the percentage of AO-positive cysts in the 150–200 μm and 200–250 μm size classes by seven-fold and 2.6-fold, respectively, compared with vehicle-treated animals. Differences in the percentage of PI-positive cysts, both among the three treatment groups and among the different cyst classes were significant ($P<0.001$). A 3-day cadmium treatment significantly ($P<0.05$) increased the percentage of PI-positive cysts in the size classes of 100–150 μm, 150–200 μm and 200–250 μm by six-fold, eight-fold and four-fold, respectively, compared with vehicle-treated animals. The interaction between treatment and cyst-size class was not significant ($P=0.142$). The mean number of AO spots per cyst also varied significantly among the three treatment groups ($P<0.001$) and among the different cyst classes ($P<0.0001$, Exp. 2, Fig. 6). The interaction between treatment and cyst-size class was borderline-significant ($P=0.0535$). A 3-day cadmium treatment significantly ($P<0.05$) increased the mean number of AO spots per cyst in the size classes of 150–200 μm and 200–250 μm by three-fold compared with vehicle-treated animals.
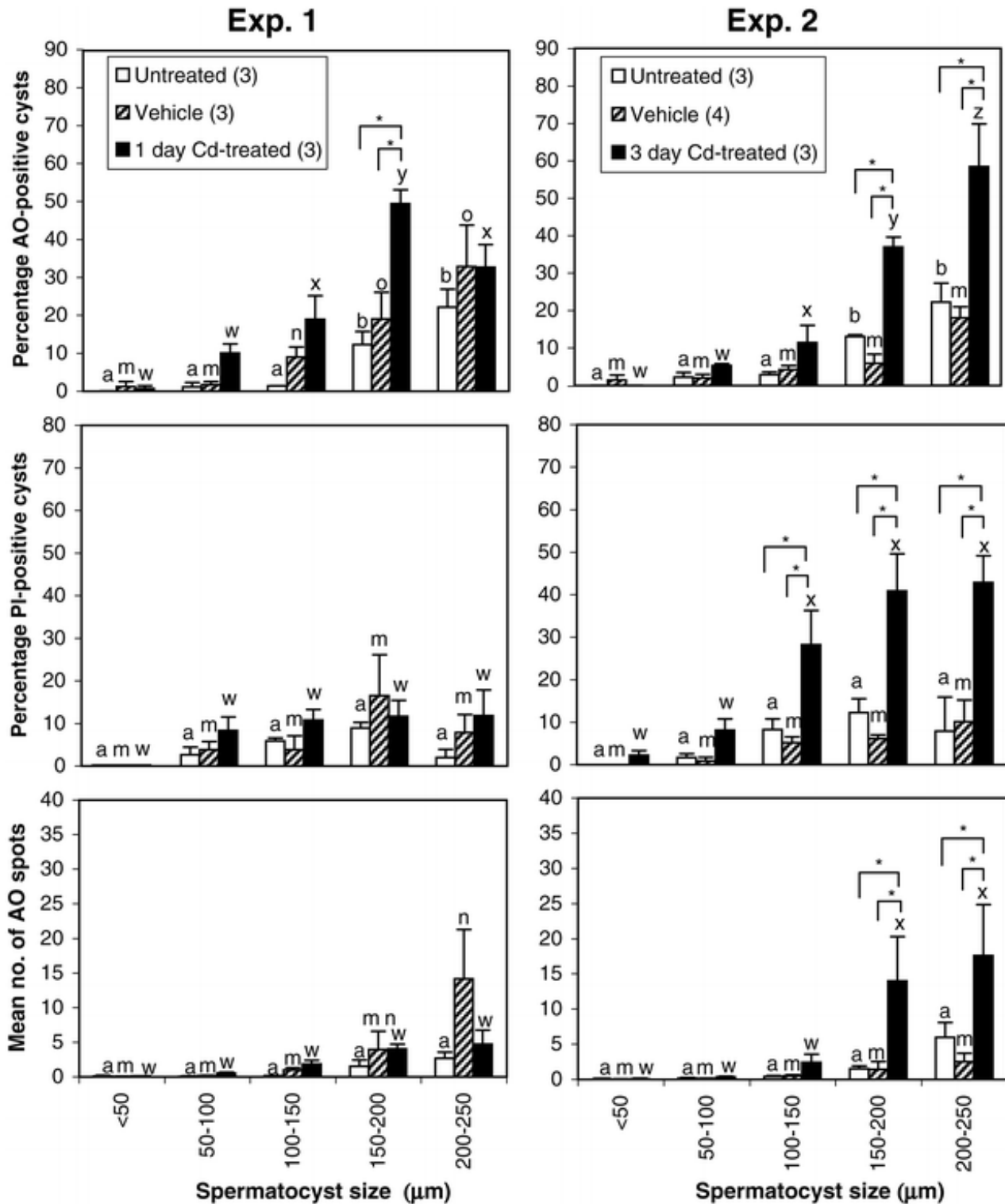
Fig. 6 Effects of $CdCl_2$ on normal stage-dependent differences in the percentage of AO-positive and PI-positive cysts and on the mean number AO spots per cyst in each PrM substage category. Animals received a single injection of $CdCl_2$ (5 mg/0.2 ml EDM per kg body weight) or vehicle or were left untreated and killed 1 day (*Exp. 1*) or 3 days (*Exp. 2*) later (*bars* mean±SEM of 3–4 animals). Raw percentage data were arcsine-square-root transformed prior to analysis by two-way ANOVA; the Student-Newman-Keuls multiple comparison test was used to identify means that differed significantly. Different *letters* indicate significant differences (*P*<0.05) among different cyst-size classes; treatment effects within a given cyst size class are indicated by *horizontal bars* (*asterisk*). **a**, **b** Untreated controls, **m-o** vehicle-treated controls, **w-z** cadmium-treated
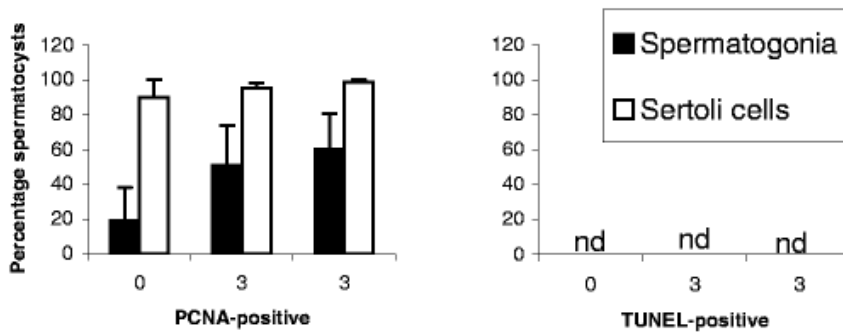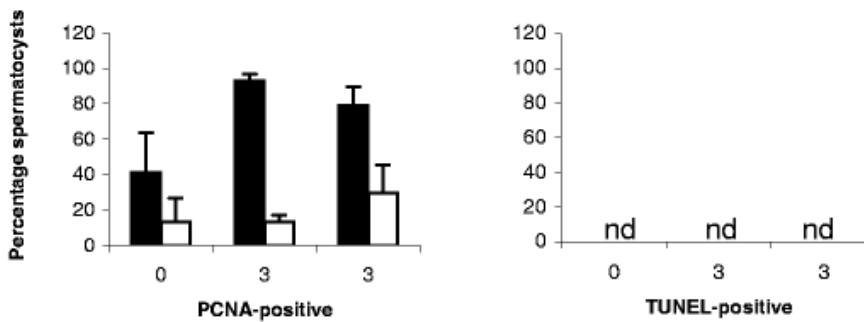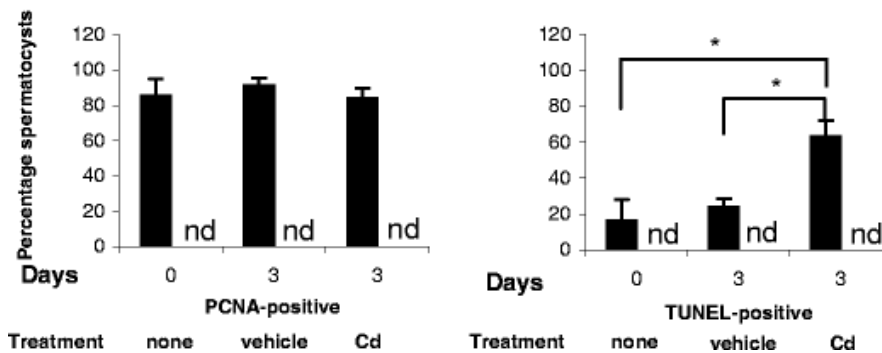
Fig. 7 Effect of CdCl$_2$ on PCNA and TUNEL immunolabelling of germ cells and Sertoli cells in paraffin sections of 3-day cadmium-treated animals. Values represent the mean percentage (±SEM) of labelled spermatocysts at a given stage. Percentages were arcsine-square-root transformed and each cyst and the cell type was analysed by two-way ANOVA for effects of treatment and time after injection. Means that differed significantly are indicated (*P<0.01, *nd* none detected)

To verify whether the increase in the percentage of PI-positive cysts in the larger cyst-size classes at 3 days post-treatment was attributable to necrosis or apoptosis, PCNA and TUNEL immunohistochemistry was perfomed on all formalin-fixed testicular cross sections of the 3-day cadmium experiment. The stage-dependent PCNA immunostaining pattern, as previously described in normal *Squalus* testis (McClusky *2005*), was not affected by 3-day cadmium treatment (Fig. 7). By contrast, the percentage of TUNEL-positive mid-stage PrM cysts (size classes of 150–250 μm) increased significantly (P<0.01) by almost three-fold compared with vehicle-treated animals. These stage-dependent effects of the 3-day cadmium treatment could also be observed in routine histology of cadmium-treated testes (not shown). The cellular organization of many mid-stage PrM cysts in cadmium-treated testes were disrupted and these cysts contained many pyknotic nuclei and vacuolated spaces. GZ, early stage PrM, M and PoM cysts in cadmium-treated testes appeared normal at the light-microscopic level, with no evidence of necrosis or inflammation (not shown). There were no marked differences between the interstitial spaces and vasculature in cadmium-treated and control testes. Further evidence that cadmium treatment did not kill the cysts is provided in Table 1. Macromolecular [³H]thymidine incorporation in PrM cysts, although showing a tendency to rise at 1 day post-treatment, remained unchanged at 3 days post-treatment.

Table 1 Effects of CdCl$_2$ treatment on macromolecular [^{3}H]thymidine incorporation in PrM cysts. Treatments were as described in Fig. 6. Values (dpm/µg protein) are expressed as mean±SEM of 3–4 animals per treatment and experiment. Means were not significantly different in both experiments

Experiment number	Treatment		
	Untreated	Vehicle	Cadmium
Exp. 1:	20.8±5.02	42.0±6.42	54.8±6.13
Exp. 2:	20.8±8.7	12.6±1.99	20.6±3.86

Effects of cadmium on blood-testis barrier function

Since the establishment of a functional blood-testis barrier was determined to be associated with postmeiotic events (Fig. 5), barrier integrity was assessed after cadmium treatment. The percentage of PoM D-R-excluding cysts was significantly ($P<0.001$) reduced after a 1-day cadmium treatment by 10% compared with vehicle-treated animals (Fig. 8, Exp. 1), and was further significantly ($P<0.01$) reduced after a 3-day cadmium posttreatment by 20% compared with vehicle-treated testes (Fig. 8, Exp. 2), suggesting a compromised privileged postmeiotic germinal compartment.
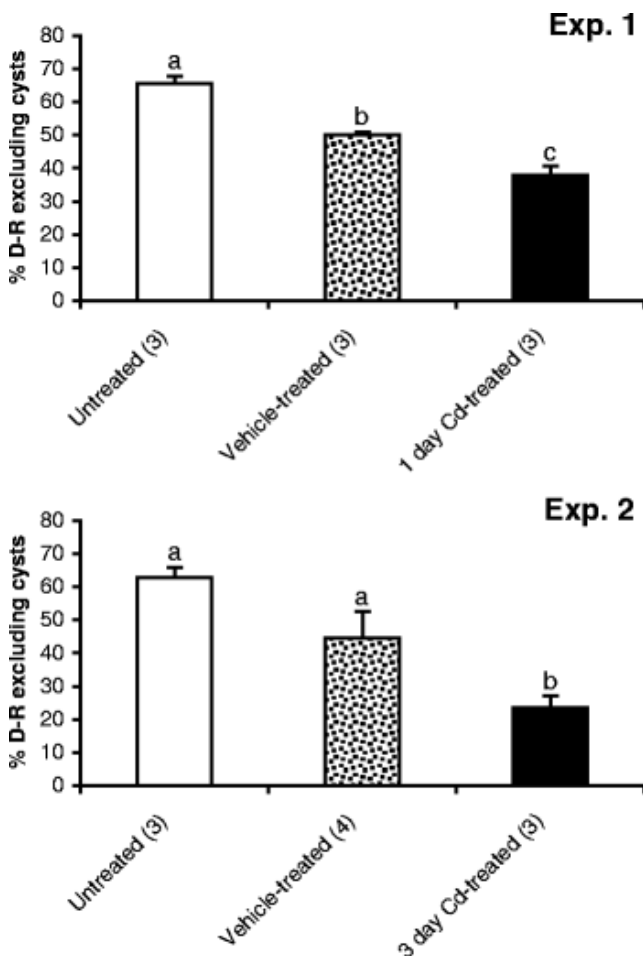
Fig. 8 Effects of CdCl$_2$ on D-R exclusion in PoM cysts (blood-testis barrier function). Results are based on the same animals that were treated in Fig. 6 (*bars* mean percentage±SEM of D-R-excluding cysts; 3–4 animals per treatment). Raw percentage data were arcsine-square-root transformed prior to analysis by one way ANOVA and the Student Newman Keuls multiple comparison test to isolate means that differed significantly. Treatment differences were significant (Exp. 1, $P<0.001$; Exp. 2, $P<0.01$). Different *letters* indicate significant differences ($P<0.05$). The mean percentage PI-positive cysts was 2±0.0021% in both experiments regardless of treatment

Discussion

Variations in the transillumination patterns of the unstained living mammalian seminiferous tubule have long been utilized to stage the mammalian seminiferous epithelium and to study the regulation of spermatogenesis accordingly (for a review, see Parvinen *1982*). Since a single mammalian Sertoli cell simultaneously nurtures four or five different germ cell stages and since each germ cell stage is known to control Sertoli cell secretory activities in a stage-related manner (Jégou et al. *1992*; Grima et al. *1998*), in vitro studies aimed at analysing testicular processes stage-by-stage are technically difficult.

The present study demonstrates the utility of an unconventional model, i.e. the shark testis, for assessing cellular processes stage-by-stage in living testicular tissue. The light and dark transillumination patterns of dispersed cysts are similar to those of other dogfish (Loir et al. *1995*). The AO vital staining method on fresh-cut testicular cross sections and staged cyst preparations has shown that specific punctate AO-labelling is limited to PrM stages and never observed in M and PoM stages, confirming the biochemical and TUNEL analyses in previous studies (Callard et al. *1995*; McClusky *2005*). Within the PrM region, there is an increasing gradient of punctate AO-labelling (mature>immature), culminating in the total AO-labelling of cysts, i.e. that of the ZD, a finding that is consistent with the TUNEL analysis (McClusky *2005*). The ZD, which is thus labelled by both the TUNEL and the AO techniques, represents the past winter's M-PrM cysts that ceased any further development (McClusky *2005*), presumably as a result of a natural break in pituitary gonadotropin support during the winter months (Simpson and Wardle *1967*; Dobson and Dodd *1977*). AO-labelling varies from discrete punctate bright green labelling (in mid-stage PrM cysts), which indicates an early stage of germ cell apoptosis, to intense yellow-orange labelling observed in flattened ZD cysts, which indicates an advanced stage of apoptosis and labelling associated with the phagocytosed germ cell corpses in Sertoli cells. Electron microscopy of AO-positive PrM and ZD cysts has confirmed the classical morphological features associated with apoptosis, i.e. separation from neighbouring cells, chromatin condensation and cell shrinking. Finally, the bright green fluorescence emitted by AO-stained PoM cysts further demonstrates that AO labels condensed chromatin. Our findings agree with those of Durrieu et al. (*1998*) who have found that the AO vital staining technique detects various stages of the apoptotic process, including stages that precede caspase activation and those during which apoptotic corpses are phagocytosed. However, in the final stage of apoptosis (also referred to as secondary necrosis; Majno and Joris *1995*) and just prior to the apoptotic cell being phagocytosed, the plasma membrane of the apoptotic cell is compromised, allowing labelling of the nucleus with PI. Nevertheless, based on the extremely low fraction of PI-labelled cysts in double-stained freshly dispersed cysts, we conclude that the dispersal procedure damages only a small percentage of cysts.

When animals were injected with a single cadmium dose (5 mg/kg) and killed 1 or 3 days later, the proportion of AO-positive cysts increased in susceptible cyst-size classes (mid-stage PrM cysts), with the effects of cadmium being more pronounced after 3 days than after 1 day of treatment. Unlike after a 1-day cadmium treatment, a 3-day treatment significantly increased the proportion of PI-positive cysts in the mid-stage PrM cysts, with the TUNEL analysis confirming the increased germ cell death in these size classes as being apoptotic; Sertoli cells were not affected. Cadmium is known to exert its effects rapidly and increases the rate of germ cell apoptosis in the rat within 12 h (Ozawa et al. *2002*). Therefore, the rate of death, as revealed by PI, might far exceed the rate of phagocytosis by the Sertoli cells, an idea that is consistent with the 10-month existence of the ZD (McClusky *2005*). Cadmium had neither an effect on PrM cyst DNA synthesis nor on PCNA immunoexpression. Moreover, since the sections lacked any histological evidence of necrotic death, we conclude that the increase in the PI index is not attributable to necrosis. The results presented here thus show that the apoptosis-promoting effects of cadmium are related to the endogenous stage-dependent gradient of apoptosis in spermatogenically active *Squalus* testes (mature PrM>immature PrM>GZ), which is the opposite of the cadmium accumulation gradient (GZ>immature PrM>mature PrM), with cadmium binding in the GZ being equivalent to that in liver (Betka and Callard *1999*).

Given the ability of the GZ to concentrate cadmium, our findings that the proliferative and apoptotic activities in the GZ and early stage PrM cysts are largely unaffected by cadmium, are thus surprising. Although PCNA immunoexpression, especially in the immature spermatogonial generations, show a tendency to increase following cadmium treatment, this may reflect unregulated DNA synthesis or DNA repair (Degraeve *1981*). This seemingly unresponsiveness of immature testicular regions to cadmium may be an evolutionary conserved trait, because testicular cadmium accumulation in rodents is five-fold higher in 4-day-old rats than in adult rats, with the neonatal rat testis also being insensitive to cadmium treatment (Wong and Klaassen *1980*). By extension, these relatively similar findings in rats and sharks suggest that the developmental and/or cell-cycle status of Sertoli cells and/or germ cells determine the sensitivity of the immature testicular region to cadmium (new Sertoli cells are formed during each spermatogenic cycle in sharks). Nevertheless, from a technical point of view, this model is useful for studying developmental aspects of cadmium toxicity in the testis, thus obviating the need for longitudinal studies required when investigating mammalian models.

Whereas the mechanism by which cadmium induces cell death in the mammalian testis is still unclear (Chiqouine and Suntzeff *1965*; Xu et al. *1996*; Sinha Hikim et al. *1997*; Ozawa et al. *2002*; Gupta et al. *2004*), the results presented here clearly show that cadmium preferentially increases the apoptotic rate in apoptosis-sensitive germ cell stages in this model. Although our findings provide no direct insight regarding the mechanism of cadmium induction of germ cell apoptosis, Betka and Callard (*1999*) have found that, although cytosolic cadmium-binding components other than heavy-metal-binding metallothionein can, to some extent, account for the cadmium accumulation gradient in the shark testis, a second nuclear-associated component of cadmium is present in larger amounts in immature than in mature spermatogonial regions in the testis of *Squalus*. Cadmium has a high affinity for nucleic acids and accumulates within the nuclear compartment, even when present in trace amounts (Snow *1992*; Hamada et al. *1994*). Nuclear-associated cadmium may displace zinc in polymerases, other metalloenzymes or transcription factors, all of which are present in larger amounts in the nuclei of proliferating cells (Din and Frazier *1985*) or it may directly induce chromatin changes (Banfalvi et al. *2005*). Interestingly, classic androgen and oestrogen receptors, both zinc-finger proteins, are concentrated in PrM regions of the shark testis (Callard et al. *1985*; Cuevas and Callard *1992*) and cadmium can reduce liver vitellogenin expression through its direct binding to oestrogen receptor-α in the trout (Vetillard and Bailhache *2005*). Furthermore, since the Sertoli cell is the sole steroid-producing element in *Squalus* (Pudney and Callard *1984*), cadmium-induced inhibition of steroidogenic activities in mid-stage PrM cysts might result in their increased apoptotic death, as is known for the rat (Ozawa et al. *2002*; Gupta et al. *2004*). Taken together, male germ cells and the complex hormonally regulated processes that support their proliferation and development may therefore be especially vulnerable to the effects of cumulative toxicants and chemicals acting as "bio-substitutes" and endocrine disrupters.

The identification of apoptosis as the mode of germ cell death in the shark testis following cadmium exposure may also be related to the protracted duration of testicular apoptosis in vertebrates with cystic spermatogenesis, such as sharks (McClusky *2005*) and teleosts (unpublished observations). The effects of high doses of cadmium may be so rapid in rodents that the terminal stage of apoptosis, also called secondary necrosis (Majno and Joris *1995*), is quickly reached, thus rendering the detection of apoptotic cells by the TUNEL method difficult (Sinha Hikim et al. *1997*; Gupta et al. *2004*). These differences further highlight the technical advantages of using a combination of a rapid vital staining technique such as AO, an early detector of apoptosis in living cells (Durrieu et al. *1998*), and this model for such studies. In addition, the criterion of using three AO-positive spots to designate a cyst as apoptotic is conservative, which further validates our findings.

We have also developed a staining method to assess the functional blood-testis barrier in the shark testis. In the D-R exclusion assay, the large (10,000 MW) D-R molecule is expected to be excluded from the germinal compartment by intact inter-Sertoli cell tight junctions in PoM cysts. Our results indicate that barrier formation in the shark is complete in PoM stages, findings that agree with those in teleost and

amphibian species with a cystic mode of spermatogenesis (Bergmann et al. *1984*). The percentage of D-R-excluding cysts is significantly reduced both 1 day and 3 days post-treatment. Although animal handling tends to have similar effects to cadmium treatment, our results, especially for the 1-day treatment experiment, extend the findings of Betka and Callard (*1999*), who have shown that the PoM-stage is able to concentrate ^{109}Cd to levels 18-fold higher than that in plasma. These results in *Squalus* also agree in principle with those of Setchell and Waites (*1970*), who, despite not demonstrating compromised barrier function, have reported increased uptake of ^{86}Rb by the adult rodent testis within 2 h after a single subcutaneous injection of CdCl$_2$. Cadmium is known to disrupt the microfilament bundles associated with the tight junctions of rat testis (Hew et al. *1993a,b*) and to induce inter-Sertoli tight junction dissasembly in cultured 20-day-old rat Sertoli cells by reducing occludin and E-cadherin expression, all of which is reversible by testosterone and follicle-stimulating hormone (Chung and Cheng *2001*). Altogether, the demonstrated ability of cadmium to gain access to the privileged compartment housing the spermatids and spermatozoa even at this phyletic level may, to some extent, explain the findings of mid-piece defects and immature forms of spermatozoa in human semen (Chia et al. *1992*).

To reiterate, the results of this study and those of Betka and Callard (*1999*) suggest that, although more mature spermatogonial generations accumulate cadmium to a lesser extent than immature spermatogonial generations, the former are more susceptible to the effects of cadmium on apoptosis. Even though the blood-testis barrier is negatively affected in PoM cysts following cadmium treatment, cadmium accumulation within PoM cysts per milligram wet weight basis does not occur to the same extent as that in stem cell and spermatogonial generations (Betka and Callard *1999*). Differences in cadmium accumulation between the PrM and PoM region may be related to the differences in cyst numbers. The absolute number of cysts in the PrM region is two-fold to three-fold higher than in the PoM region (McClusky *2005*). Nevertheless, the potential for cadmium interference in the normal spermatogenic progression is substantial, because of the steroid-mediated regulation of the process and the high levels of DNA synthesis and gene transcription, all of which are processes in which zinc is integrally involved (Snow *1992*).

In conclusion, our results show that cadmium (1) targets early spermatogenic stages, where it specifically activates a cell death program in susceptible (mature) spermatogonial clones, and (2) negatively affects blood-testis barrier function. Further studies are required to determine whether germ cells or Sertoli cells are primary cadmium targets in effects on these processes. Since other parameters measured here are relatively unaffected by cadmium, this indicates that the effects of this toxicant on apoptosis are process-specific and not attributable to general toxicity.

References

Abrams JM, White K, Fessler I (1993) Programmed cell death during *Drosophila* embryogenesis. Development 117:29–43

Banfalvi G, Gacsi M, Nagy G, Kiss ZB, Basnakian AG (2005) Cadmium induced apoptotic changes in chromatin structure and subphases of nuclear growth during the cell cycle in CHO cells. Apoptosis 10:631–642

Bergmann M, Schindelmeiser J, Greven H (1984) The blood-testis barrier in vertebrates having different testicular organization. Cell Tissue Res 238:145–150

Betka M, Callard GV (1999) Stage-dependent accumulation of cadmium and induction of metallothionein-like binding activity in the testis of the dogfish shark, *Squalus acanthias*. Biol Reprod 60:14–22

Broaddus VC, Yang L, Scavo LM, Ernst JD, Boylan AM (1996) Asbestos induces apoptosis of human and rabbit pleural mesothelial cells via reactive oxygen species. J Clin Invest 98:1–10

Callard GV, Pudney JA, Mak P, Canick J (1985) Stage-dependent changes in steroidogenic enzymes and estrogen receptors during spermatogenesis in the testis of the dogfish *Squalus acanthias*. Endocrinology 117:1328–1335

Callard GV, Jorgensen JC, Redding JM (1995) Biochemical analysis of programmed cell death during premeiotic stages of spermatogenesis in vivo and in vitro. Dev Gen 16:140–147

Chia SE, Ong CN, Lee ST, Tsakok FH (1992) Blood concentrations of lead, cadmium, mercury, zinc, and copper and human semen parameters. Arch Androl 29:177–183

Chiqouine AD, Suntzeff V (1965) Sensitivity of mammals to cadmium necrosis of the testis. J Reprod Fertil 10:455–457

Choe S, Kim S, Kim H, Lee JH, Choi Y, Lee H, Kim Y (2003) Evaluation of estrogenicity of major heavy metals. Sci Tot Environ 312:15–21

Chung NPY, Cheng CY (2001) Is cadmium chloride-induced inter-Sertoli tight junction permeability barrier disruption a suitable in vitro model to study the events of junction disassembly during spermatogenesis in the rat testis? Endocrinology 142:1878–1888

Cuevas ME, Callard GV (1992) Androgen and progesterone receptors in shark (*Squalus*) testis: characteristics and stage-related distribution. Endocrinology 130:2173–2182

Degraeve N (1981) Carcinogenic, teratogenic and mutagenic effects of cadmium. Mut Res 86:115–135

Din WS, Frazier JM (1985) Protective effect of metallothionein on cadmium toxicity in isolated rat hepatocytes. Biochem J 230:395–402

Dobson S, Dodd JM (1977) Endocrine control of the testis in the dogfish *Scyliorhinus canicula* L. II. Histological and ultrastructural changes in the testis after partial hypophysectomy (ventral lobectomy). Gen Comp Endocrinol 32:53–71

DuBois W, Callard GV (1991) Culture of intact Sertoli/germ cells units and isolated Sertoli cells from *Squalus* testis. I. Evidence of stage-related functions in vitro. J Exp Zool 258:359–372

DuBois W, Callard GV (1993) Culture of intact Sertoli/germ cell units and isolated Sertoli cells from *Squalus* testis. II. Stimulatory effects of insulin and IGF-I on DNA synthesis in premeiotic stages. J Exp Zool 267:233–244

Durrieu F, Belloc F, Lacoste L, Dumain P, Chabrol J, Dachary-Prigent J, Morjani H, Boisseau MR, Reiffers J, Bernard P, Lacombe F (1998) Caspase activation is an early event in anthracycline-induced apoptosis and allows detection of apoptotic cells before they are ingested by phagocytes. Exp Cell Res 240:165–175

Dym M, Fawcett DW (1970) The blood-testis barrier in the rat and the physiological compartmentation of the seminiferous epithelium. Biol Reprod 3:308–326

Grima J, Wong CC, Zhu LJ, Zong SD, Cheng CY (1998) Testin secreted by Sertoli cells is associated with the cell surface, and its expression correlates with the disruption of Sertoli-germ cell junctions but not the inter-Sertoli tight junction. J Biol Chem 273:21040–21053

Gupta RS, Kim J, Gomes C, Oh S, Park J, Seong JY, Ahn RS, Kwon H, Soh J (2004) Effect of ascorbic acid supplementation on testicular steroidogenesis and germ cell cell death in cadmium-treated male rats. Mol Cell Endocrinol 221:57–66

Hamada T, Tanimoto A, Iwai S, Fujiwara H, Sasaguri Y (1994) Cytopathological changes induced by cadmium-exposure in canine proximal tubular cells: a cytochemical and ultrastructural study. Nephron 68:104–111

Hechtenberg S, Schafer T, Benters J, Beyersmann D (1996) Effects of cadmium on cellular calcium and proto-oncogene expression. Ann Clin Lab Sci 26:512–521

Hew KW, Heath GL, Jiwa AH, Welsh MJ (1993a) Cadmium in vivo causes disruption of tight junction-associated microfilaments in rat Sertoli cells. Biol Reprod 49:840–849

Hew KW, Ericson WA, Welsh MJ (1993b) A single low cadmium dose causes failure of spermiation in the rat. Toxicol Appl Pharmacol 121:15–21

Hjollund NHI, Bonde JPE, Jensen TK, Ernst E, Henriksen TB, Kolstad HA, Giwercman A, Skakkebaek NE, Olsen J (1998) Semen quality and sex hormones with reference to metal welding. Reprod Toxicol 12:91–95

Jégou B, Pineau C, Vélez de la Calle J, Bardin W, Touzalain AM, Cheng CY (1992) Germ cell control on testin production is inverse to that of other Sertoli cell parameters. Endocrinology 132:2557–2562

Loir M, Sourdaine P, Mendis-Handagama SMLC, Jégou B (1995) Cell-cell interactions in the testis of teleosts and elasmobranchs. Microsc Res Tech 32:533–552

Lowry OH, Rosebrough NJ, Farr AL, Randall RJ (1951) Protein measurement with the Folin phenol reagent. J Biol Chem 193:265–275

Majno G, Joris I (1995) Apoptosis, oncosis, and necrosis. Am J Pathol 146:3–15

McClusky LM (2005) Stage and season effects on cell cycle and apoptotic activities of germ cells and Sertoli cells during spermatogenesis in the spiny dogfish (*Squalus acanthias*). Reproduction 129:89–102

Oldereid NB, Thomassen Y, Attramadal A, Olaisen B, Purvis K (1993) Concentrations of lead, cadmium and zinc in the tissues of reproductive organs of men. J Reprod Fertil 99:421–442

Ortego LS, Hawkins WE, Walker WW, Kroll RM, Benson WH (1994) Detection of proliferating cell nuclear antigen in tissues of three small fish species. Biotech Histochem 69:317–323

Ozawa N, Goda N, Makino N, Yamaguchi T, Yoshimura Y, Suematsu M (2002) Leydig cell-derived heme oxygenase-1 regulates apoptosis of premeiotic germ cells in response to stress. J Clin Invest 109:457–467

Parvinen M (1982) Regulation of the seminiferous epithelium. Endocr Rev 3:404–417

Pudney J, Callard GV (1984) Identification of Leydig-like cells in the interstitium of the shark testis (*Squalus acanthias*). Anat Rec 209:311–330

Setchell BP, Waites GMH (1970) Changes in the permeability of the testicular capillaries and of the "blood testis barrier" after injection of cadmium chloride in the rat. J Endocrinol 47:81–86

Sever LE (1997) Epidemiologic evidence for toxic effects of occupational and environmental chemicals on the testes. In: Thomas JA, Colby HD (eds) Endocrine toxicology, 2nd edn. Taylor and Francis, Washington London, pp 287–326

Simpson TH, Wardle CS (1967) A seasonal cycle in the testis of the spurdog, *Squalus acanthias*, and the sites of 3β-hydroxysteroid dehydrogenase activity. J Mar Biol Assoc UK 47:699–708

Sinha Hikim AP, Lue Y, Swerdloff RS (1997) Separation of germ cell apoptosis from toxin-induced cell death by necrosis using in situ-labelling histochemistry after glutaraldehyde fixation. Tissue Cell 29:487–493

Snow ET (1992) Metal carcinogenesis: mechanistic implications. Pharmacol Ther 53:31–65

Sundaram K, Witorsch RJ (1995) Toxic effects on the testes. In: Witorsch RJ (ed) Reproductive toxicology. Raven, New York, pp 99–224

Vetillard A, Bailhache T (2005) Cadmium: an endocrine disrupter that affects gene expression in the liver and brain of juvenile rainbow trout. Biol Reprod 72:119–126

Wong K-L, Klaassen CD (1980) Age difference in the testicular susceptibility to cadmium-induced testicular damage in rats. Toxicol Appl Pharmacol 55:456–466

Xu C, Johnson JE, Singh PK, Jones MM, Yan H, Carter CE (1996) In vivo studies of cadmium-induced apoptosis in testicular tissue of the rat and its modulation by a chelating agent. Toxicology 107:1–8